IJARCCE ISSN (O) 2278-1021, ISSN (P) 2319-5940

International Journal of Advanced Research in Computer and Communication Engineering

Impact Factor 8.471 ⁜ Peer-reviewed & Refereed journal ⁜ Vol. 15, Issue 5, May 2026

DOI: 10.17148/IJARCCE.2026.155248

Micro-Grid Energy Management Using Inverters

Manoj Gowda B P[1], B J Jayadeva[2], Prajwal H R[3], Vaibhav S[4]

Student, Electrical and Electronics Engineering Dept., PESCE, Mandya, India[1-4]

Abstract: This paper presents a control strategy for a solar PV–battery micro-grid using both grid-following (GFL) and grid-forming (GFM) inverters. GFL uses PLL and vector control but lacks support during grid outages. GFM, based on a virtual synchronous machine, provides voltage/frequency control, islanding, and fault ride-through capabilities. A 100 MW PV and 60 MW BESS system was simulated and validated experimentally. GFM improved system frequency by 69.3% and voltage by 70%, significantly outperforming GFL.

Keywords: grid-forming inverter; grid-following inverter; fault ride-through capability; microgrid; photovoltaic energy; power electronics

I. INTRODUCTION

The modern power system is increasingly facing stability challenges as the penetration of inverter-based renewable resources (IBRs) continues to grow, leading to a significant reduction in overall system inertia [1,2]. The gradual replacement of conventional synchronous generators with renewable energy sources has altered the dynamic characteristics of the grid. In particular, the displacement of synchronous machines results in reduced synchronization torque, lower inertial response, and limited short-circuit current capability, all of which pose critical challenges for IBR- dominated power systems [3]. Moreover, the inherent intermittency of renewable energy generation introduces frequent voltage and frequency fluctuations, further complicating stable grid operation.

The primary challenges associated with high IBR penetration can be summarized as follows:

(a) degradation of grid strength and reduced short-circuit current levels, which adversely affect system stability and protection coordination;

(b) diminished system inertia, leading to increased vulnerability to frequency instability;

(c) the ability to Establishing and maintaining grid voltage and frequency without synchronous generators is crucial, especially during reliable grid restoration and black-start capability after large outages. Renewable energy sources usually connect to the power grid through two main inverter control strategies: grid- following (GFL) and grid-forming (GFM) inverters. In the past decade, most grid-connected renewable installations have used GFL inverters. These inverters depend on externally defined grid voltage and frequency references. Because they rely on grid conditions and communication-based measurements, GFL inverters have a limited response to rapid system disturbances. As the number of inverter-based resources (IBRs) grows, inverter control strategies must change to respond better to faster system dynamics and help improve power system stability.

A GFL inverter works as a controlled current source that aligns with the grid voltage using appropriate control mechanisms. However, GFL inverters cannot provide inertial support since they do not mimic the dynamic behavior of synchronous generators. Unlike synchronous machines, which can adjust their output in response to frequency changes, GFL inverters usually operate at set power points. GFL inverters achieve synchronization through a phase- locked loop (PLL), which estimates the grid's phase angle and frequency needed to align the inverter output with the grid. The GFL control architecture typically includes two cascaded loops: a slower outer voltage control loop and a faster inner current control loop. Because of this design, GFL inverters cannot directly regulate system voltage and frequency, making it difficult to operate effectively during severe voltage or frequency instability.

To address these limitations, the concept of grid-forming (GFM) inverters has gained considerable research interest in recent years. IBRs equipped with GFM control are capable of actively establishing and regulating grid voltage and frequency by operating as controlled voltage sources with predefined magnitude, phase angle, and frequency. This enables GFM-based IBRs to support the power system under both normal and faulted conditions, including islanded operation. The key advantages of GFM-controlled IBRs include: (a) faster control response compared to GFL inverters for maintaining voltage and frequency; (b) enhanced contribution to overall system stability; (c) provision of synchronizing and damping torque similar to synchronous generators; and (d) reduced rate of change of frequency (RoCoF) and inherent black-start capability.

IJARCCE ISSN (O) 2278-1021, ISSN (P) 2319-5940

International Journal of Advanced Research in Computer and Communication Engineering

Impact Factor 8.471 ⁜ Peer-reviewed & Refereed journal ⁜ Vol. 15, Issue 5, May 2026

DOI: 10.17148/IJARCCE.2026.155248

Maintaining synchronous generators online during grid disturbances is costly and difficult to manage. Energy storage systems (ESS) have emerged as a practical and efficient alternative to support grid stability. Recently, there has been a lot of research on the control strategies for grid- following (GFL) inverters. Grid-forming (GFM) inverters have also gained significant attention due to their ability to provide independent voltage and frequency support. In [14], a droop-controlled GFM inverter is compared to a frequency- support-based GFL inverter under different levels of renewable penetration and system inertia. The study shows that frequency-controlled GFL inverters often show less damping and greater frequency deviations. On the other hand, systems using GFM inverters demonstrate better frequency damping and a smoother handling of overload conditions among available sources, which improves overall system reliability.

The performance of GFL and GFM inverters in a low-inertia power system with a battery energy storage system (BESS) is explored in [15]. Multiple case studies show that GFM- based control provides better frequency regulation than GFL- based methods. Additionally, the work in [16] looks at the basic differences between GFM and GFL inverters, focusing on synchronization methods, grid-interfacing behavior, swing dynamics, control gain characteristics, grid strength adaptability, and transient stability. Findings in [17] reveal that adding voltage control features can significantly lessen post-fault voltage fluctuations, which in turn improves the active power response of virtual-inertia-based GFL inverters.

The concept of the virtual synchronous generator (VSG), introduced in [18], is designed to reduce frequency instability in power systems with a heavy presence of inverter-based resources (IBRs). A thorough simulation- based evaluation of a GFM inverter controller is provided in [19]. It shows that this controller effectively stabilizes voltage and frequency while consistently supplying power to critical loads during long outages. Moreover, a detailed review in [20] classifies GFM inverter technologies into droop-based, VSG-based, compensated generalized VSG (CGVSG)-based, and adaptive VSG (AVSG)-based control schemes, comparing their performance and durability across various operating conditions.

Recent studies, such as [21], examine the behavior of GFM- based power converters in photovoltaic (PV) systems during faults. Even though GFM inverters are increasingly used in micro-grid applications with diverse topologies and configurations, technical and operational challenges persist before they can completely replace synchronous machines at the transmission level. Major research gaps include developing reliable hardware and software platforms, creating standardized inverter models, integrating large-scale renewables, coordinating energy storage, assessing system- level stability, establishing black-start capability, devising dynamic islanding strategies, meeting networking requirements, and implementing economic dispatch methods. These challenges and ongoing research topics regarding GFM inverters in micro-grid settings are thoroughly discussed in [22–26].

II. METHODOLOGY

PROBLEM STATEMENT

The integration of Renewable Energy Sources (RES) into micro-grids introduces challenges in maintaining stability and effective power management due to their intermittent nature and reliance on inverter-based interfaces. Grid-Forming (GFM) and Grid-Following (GFL) inverters play crucial roles in addressing these challenges, with GFM inverters providing voltage and frequency support, while GFL inverters depend on an established grid. However, poor coordination between them can lead to instability and inefficient power sharing. This project focuses on analyzing and optimizing the operation of GFM and GFL inverters to enhance the stability, reliability, and power management of RES-based micro-grids under varying operating conditions.

Block Diagram of a Solar–Wind Based Micro-grid:

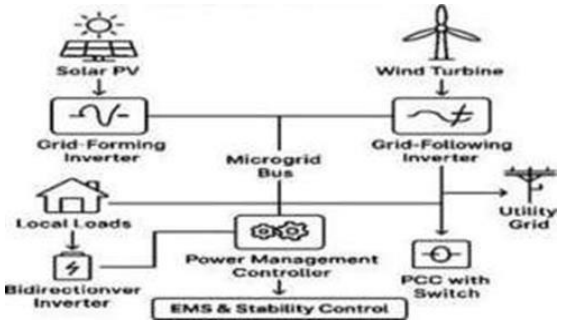

Fig 1. Block Diagram of a Solar-Wind based Micro-grid.

IJARCCE ISSN (O) 2278-1021, ISSN (P) 2319-5940

International Journal of Advanced Research in Computer and Communication Engineering

Impact Factor 8.471 ⁜ Peer-reviewed & Refereed journal ⁜ Vol. 15, Issue 5, May 2026

DOI: 10.17148/IJARCCE.2026.155248

PROPOSED FRAMEWORK OF COORDINATED CONTROL OF GFL AND GFM INVERTERS

In inverter-based, renewable-dominated power systems, the gradual replacement of synchronous generators with inverter-interfaced photovoltaic (PV) sources introduces significant operational challenges. The reduction in synchronous generation leads to lower system inertia and reduced synchronizing torque, making the grid more susceptible to voltage and frequency variations. These effects are further intensified by the intermittent nature of inverter-fed PV generation.

To address these challenges, the proposed inverter-based resource (IBR) control framework integrates two complementary control strategies within renewable-fed inverters: grid-following (GFL) control and grid-forming (GFM) control. In this work, the stability of the power system is analyzed by interfacing solar PV systems with the grid through GFL inverter control, while battery energy storage systems (BESS) are connected using GFM inverter control. The GFL inverters operate by synchronizing with the existing grid and injecting controlled active and reactive power, whereas the GFM inverter establishes and regulates system voltage and frequency, thereby providing essential inertial and stabilizing support.

The coordinated operation of GFL and GFM inverters enables improved voltage and frequency regulation, enhanced power sharing, and increased system robustness under varying operating conditions. A schematic representation of the coordinated GFL and GFM control architecture within the micro-grid is presented in the corresponding diagram.

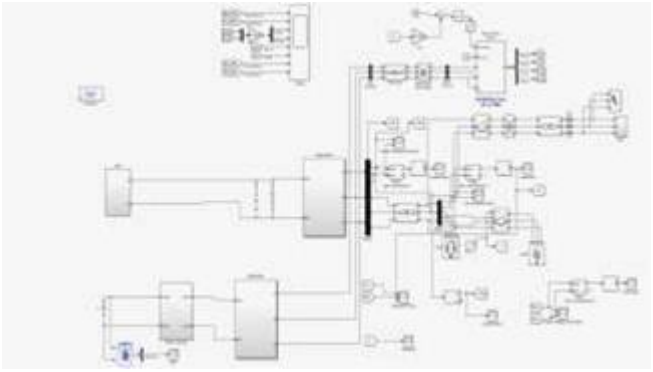

Fig 2. Scheduled diagram of GFL & GFM inverter control in PV- BESS-integrated microgrid.

As shown in Fig. 2, the grid-following (GFL) inverter operates in current control mode and comprises an outer synchronization loop and an inner current control loop. The GFL inverter synchronizes with the grid by tracking the phase angle of the voltage at the point of common coupling (PCC). Using a vector control strategy, it regulates the active and reactive current components injected into the grid based on grid reference values.

In contrast, the grid-forming (GFM) inverter operates in voltage control mode and is responsible for establishing the reference voltage magnitude and frequency of the grid. GFM-based control becomes essential during disturbed network conditions, such as system faults or islanded operation, where conventional grid references are unavailable or unreliable. Under these conditions, the GFM inverter actively regulates voltage and frequency, enhances grid strength, and ensures stable operation even in scenarios with high penetration of inverter-based resources (IBRs). Figure 2 presents the structural overview of coordinated GFL- and GFM-based inverter control within the micro-grid.

(a) GFL-Based Inverter Control for Solar PV

The grid-following inverter control architecture for the solar PV system is illustrated in Fig. 3. This control structure consists of a phase-locked loop (PLL) and an inner current control loop to regulate the inverter output currents. An active–reactive power (PQ) control strategy is implemented in the outer control loop to manage the power injected into the grid.

In GFL-based control, grid voltage measurements are required to obtain synchronization information. The PLL provides the reference phase angle, θ, by tracking the grid voltage at the PCC, which serves as the basis for generating reference waveforms. The outer power control loop determines the reference active and reactive power, while the inner current control loop ensures accurate tracking of the corresponding reference currents by the inverter.

Additionally, low-voltage ride-through (LVRT) capability is incorporated into the GFL inverter-fed PV system to enhance grid support during fault conditions. When a voltage dip occurs due to system disturbances, the LVRT

IJARCCE ISSN (O) 2278-1021, ISSN (P) 2319-5940

International Journal of Advanced Research in Computer and Communication Engineering

Impact Factor 8.471 ⁜ Peer-reviewed & Refereed journal ⁜ Vol. 15, Issue 5, May 2026

DOI: 10.17148/IJARCCE.2026.155248

mechanism is activated, enabling the inverter to inject adequate reactive power into the grid. This feature helps maintain voltage stability and supports overall system reliability during and after fault events.

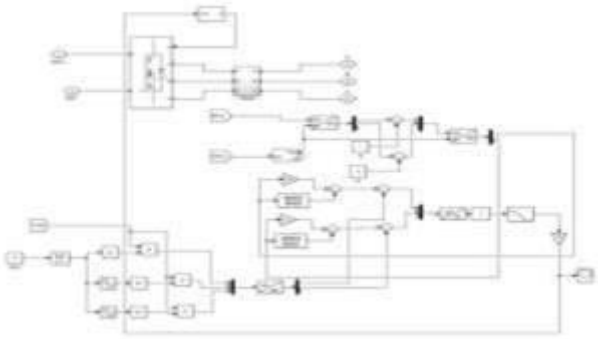

Fig. 3 Block diagram of GFL Inverter

The block diagram representation of GFL-based inverter control is shown in Figure 4.

As illustrated in Fig. 3, the measured grid-side voltage and frequency are supplied as inputs to the grid-following (GFL) inverter control algorithm. These measurements enable accurate synchronization and ensure proper interaction between the inverter and the grid. The corresponding block diagram representation of the GFL- based inverter control is presented in Fig. 4.

The control inputs to the inverter model include reference values for active power and reactive power, along with voltage and frequency references. Based on these inputs, the controller estimates the instantaneous active and reactive power exchanged with the grid and generates the corresponding reference current components. These reference currents are then used by the inner current control loop to regulate the inverter output, ensuring that the desired power is accurately injected into the grid while maintaining stable operation under varying grid conditions.

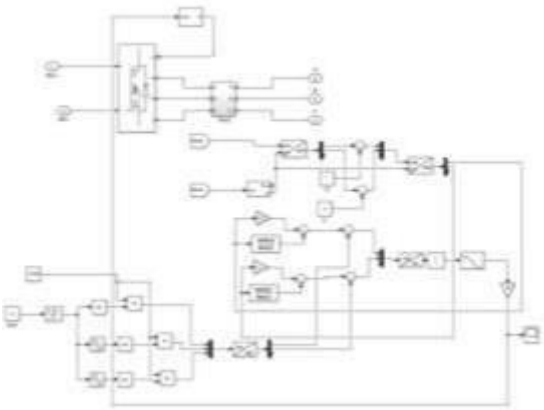

Fig. 4 GFL-based inverter control for solar PV system

(a) Virtual Synchronous Machine–Based Grid-Forming Inverter Control for BESS

As shown in Fig. 4, the grid-forming (GFM) inverter control is based on a virtual synchronous machine (VSM) concept, which is employed to regulate the voltage and frequency of the power system. In addition to voltage and frequency regulation, the control structure incorporates active and reactive power control loops to significantly enhance the dynamic performance of the system. In this study, the GFM- based inverter control is implemented for the battery energy storage system (BESS), as illustrated in the flow diagram presented in Fig. 5.

The VSM-based control strategy provides an alternative approach to grid synchronization by emulating the dynamic behavior of conventional synchronous machines, which naturally synchronize with the grid. By replicating this behavior, the VSM actively contributes to frequency stabilization during transient and dynamic operating conditions. The proposed VSM model is capable of operating in grid-connected mode, as depicted in Fig. 6, and relies solely on locally measured electrical quantities, unlike traditional synchronous generators that depend on external excitation systems.

IJARCCE ISSN (O) 2278-1021, ISSN (P) 2319-5940

International Journal of Advanced Research in Computer and Communication Engineering

Impact Factor 8.471 ⁜ Peer-reviewed & Refereed journal ⁜ Vol. 15, Issue 5, May 2026

DOI: 10.17148/IJARCCE.2026.155248

Furthermore, the virtual inertia embedded in the VSM enables effective frequency support and improves power-sharing performance during disturbances. The dominant dynamics of the synchronous machine are captured through the swing equation, which is adapted within the VSM framework. A key distinction of the VSM-based control is that it does not rely on tracking predefined reference currents or voltages. Instead, the inverter behaves as a controllable voltage source with inertial characteristics. This virtual synchronous generator (virtual SG) approach enhances short-term frequency stability and strengthens overall grid resilience under high inverter- based resource penetration.

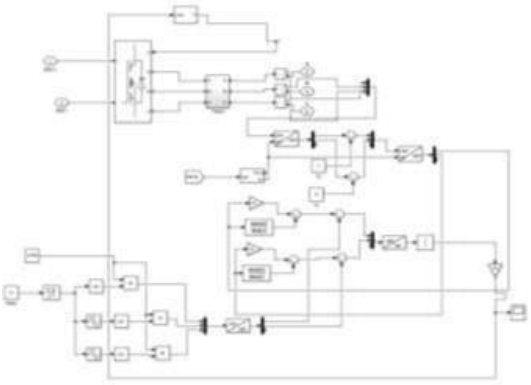

Fig. 5 Block diagram of GFM Inverter.

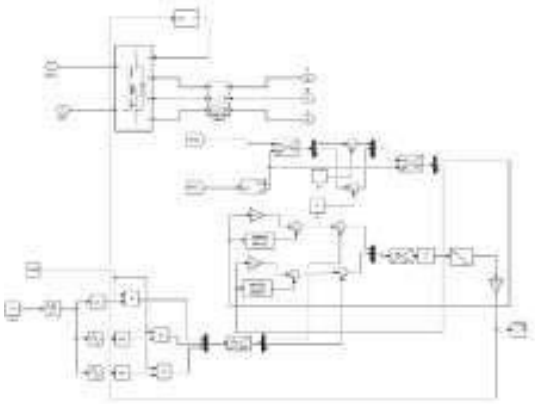

Fig. 6 GFM-based inverter control for BESS

As illustrated in Figs. 5 and 6, active power regulation in the BESS is achieved using the virtual synchronous machine (VSM)–based control strategy. In this approach, the reference phase angle of the inverter output voltage is generated to control the active power exchanged with the grid. The control algorithm is defined by two key state variables, namely the phase angle (θ) and angular frequency (ω), which are used to formulate the state-space equations governing the controller dynamics.

The dynamic behavior of the VSM is described by the swing equation, as presented in Equation (1). In this equation, ω_ref denotes the reference frequency, P_meas represents the active power delivered by the inverter, P_ref is the active power reference, and P_m corresponds to the mechanical power equivalent of the virtual machine. By emulating the swing dynamics of a synchronous generator, the VSM-based inverter adjusts the phase angle of the inverter voltage, thereby enabling effective active power control for the BESS and contributing to improved frequency stability during system disturbances.

Reactive power droop control is employed to regulate the inverter terminal voltage by adjusting the magnitude of the reference voltage of the BESS inverter. The voltage reference is determined using the droop relationship given in Equation:

$$V_d = V_{ref} + k_p(Q_e - Q_{ref})$$

Where Vref and Qref represent the reference voltage and reactive power set points of the droop controller, respectively, and Qe denotes the reactive power output of the BESS inverter. Through this control strategy, the BESS effectively

IJARCCE ISSN (O) 2278-1021, ISSN (P) 2319-5940

International Journal of Advanced Research in Computer and Communication Engineering

Impact Factor 8.471 ⁜ Peer-reviewed & Refereed journal ⁜ Vol. 15, Issue 5, May 2026

DOI: 10.17148/IJARCCE.2026.155248

supports voltage regulation and mitigates high-frequency power fluctuations. In addition, the energy storage system contributes to system stabilization by providing fast dynamic support following grid disturbances or fault conditions.

(b) PLL-Based Grid Synchronization

Grid synchronization is achieved by regulating the terminal voltage of the PV inverter such that its phase angle, magnitude, and frequency are aligned with the grid voltage at the point of common coupling (PCC), in accordance with the requirements of IEEE Std. 1547-2018 [7]. In this study, two synchronization mechanisms are utilized: a conventional phase-locked loop (PLL) to extract the phase angle of the grid voltage at the PCC, and a power-balance-based synchronization method to regulate the system frequency.

The phase detector within the PLL generates an error signal proportional to the phase difference between the reference grid voltage and the voltage produced by the internal oscillator of the PLL. This signal is processed through a loop filter, typically implemented as a first-order low-pass filter or a proportional–integral (PI) controller, which suppresses high-frequency components and ensures smooth tracking of grid voltage dynamics.

The grid-connected PV–BESS micro-grid considered in this study comprises two three-phase central inverters interfacing a solar photovoltaic plant and an energy storage system. The PV system is rated at 100 MW under standard test conditions, corresponding to an operating temperature of 25 °C and solar irradiance of 1000 W/m². The BESS has an energy storage capacity of 60MWh and is interfaced through a grid-forming inverter.

Both PV and BESS inverters are connected to a medium- voltage distribution network via a 4 kV/24.9 kV step-up transformer. The single-line diagram of the overall test system is presented in Fig. 8. The PV array is operated at its maximum power point by regulating the dc-link voltage to its reference value, thereby ensuring optimal energy extraction under varying irradiance conditions.

The proposed control framework is evaluated under both normal and disturbed operating conditions, including load variations, grid outages, solar power fluctuations, and temporary as well as permanent fault scenarios. The inverter control parameters are designed in accordance with the guidelines provided in IEEE Std. 2800 [27]. During voltage or frequency ride-through events, the proposed controller dynamically generates appropriate reference currents for the PV inverter to ensure grid support and system stability.

The test system is implemented with coordinated grid- following control for the solar PV inverters and grid-forming control for the energy storage system. The effectiveness of the proposed approach is assessed by comparing the performance of grid-following and grid-forming inverter control strategies on the BESS side across multiple case studies. The results demonstrate the superior dynamic response and stability contribution of grid-forming control, particularly under low-inertia and faulted grid conditions.

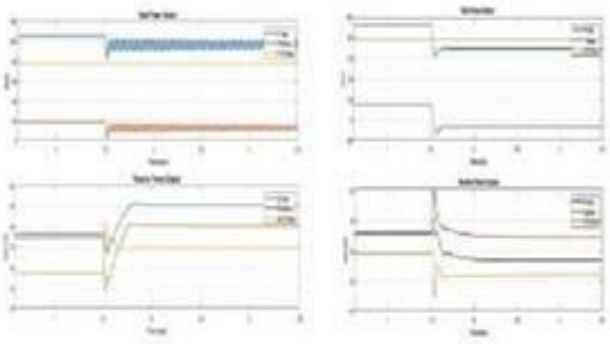

Fig 7. Performance of the system under (a) GFL and (b) GFM-based inverter control.

Case 1: Impact of Solar PV Penetration Variations under Grid-Connected Operation

This case study evaluates the dynamic performance of the proposed micro-grid by comparing grid-forming (GFM) and grid-following (GFL) control strategies implemented on the BESS inverter, while the solar PV system operates under GFL control. Variations in solar irradiance introduce fluctuations in power injection, which can disturb key system parameters and adversely affect overall stability.

IJARCCE ISSN (O) 2278-1021, ISSN (P) 2319-5940

International Journal of Advanced Research in Computer and Communication Engineering

Impact Factor 8.471 ⁜ Peer-reviewed & Refereed journal ⁜ Vol. 15, Issue 5, May 2026

DOI: 10.17148/IJARCCE.2026.155248

To assess the system response, the developed model is subjected to dynamic changes in solar PV penetration, and the resulting voltage and frequency profiles are analyzed for both inverter control strategies at the BESS side. The simulation results are presented in Fig. 9. It is observed that the voltage at the point of common coupling (PCC) is effectively regulated and settles at approximately 0.99pu within a response time of about 300ms.

A clear improvement in frequency dynamics is achieved when the BESS operates under GFM control. The system frequency stabilizes within 300 ms, with noticeably reduced switching transients compared to the GFL-controlled case. The enhanced performance of the GFM-controlled BESS can be attributed to its ability to provide virtual inertia and damping support during irradiance-induced disturbances, enabling a faster and smoother system response.

Overall, the results demonstrate that GFM inverter control significantly mitigates transient oscillations during switching events and maintains voltage and frequency within permissible limits under varying solar PV conditions. Furthermore, Fig. 10 illustrates the rate of change of frequency (RoCoF) for different inverter control strategies, highlighting the superior frequency containment achieved with GFM-based control.

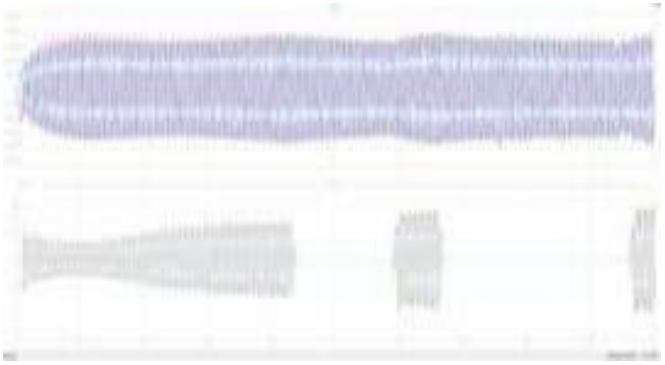

Fig 8. Performance of the system under GFL and GFM-based

Case 2: System Performance under Varying Load Conditions in Grid-Connected Mode

The dynamic performance of the proposed micro-grid is further evaluated under varying demand conditions by introducing sudden load-switching events in the medium- voltage network. In this scenario, the responses of the BESS-fed inverter operating under grid-following (GFL) and grid- forming (GFM) control strategies are compared during a step increase in load demand, as illustrated in Fig. 9.

The simulation results indicate that the BESS inverter employing GFM control responds significantly faster to load variations than the GFL-controlled inverter. Upon a sudden increase in demand, the GFM-based BESS promptly supplies the required active and reactive power, thereby supporting system stability. The voltage profile is restored within approximately 100 ms, while frequency regulation is achieved within 200ms. In contrast, the GFL-controlled inverter exhibits a slower dynamic response and larger transient deviations. These observations highlight the superior capability of GFM control in maintaining voltage and frequency stability during abrupt load changes in grid-connected operation.

Case 3: Grid Outage and Transition to Islanded Operation

This case study examines the system behavior during a grid outage that forces the micro-grid to operate in islanded mode. A three-phase fault is applied on the grid side at 1.5 s, and the response of the BESS equipped with a GFM inverter is analyzed during the transition and subsequent islanded operation.

The simulation results demonstrate that the GFM-controlled BESS successfully assumes the role of grid support by supplying the necessary power to meet the medium-voltage load demand in islanded mode. The system exhibits a rapid dynamic response, with voltage and frequency stabilization achieved within approximately 60 ms, while remaining within the acceptable limits prescribed by IEEE standards. Furthermore, during and after the fault, the GFM-based control significantly reduces switching transients and enables faster settling of system variables compared to the GFL-controlled approach. These results confirm the effectiveness of GFM inverter control in enhancing micro-grid resilience and ensuring stable operation during grid outages and fault conditions.

IJARCCE ISSN (O) 2278-1021, ISSN (P) 2319-5940

International Journal of Advanced Research in Computer and Communication Engineering

Impact Factor 8.471 ⁜ Peer-reviewed & Refereed journal ⁜ Vol. 15, Issue 5, May 2026

DOI: 10.17148/IJARCCE.2026.155248

Fig 9. Waveforms of the GFL, GFM & Solar Power.

Figure 9 illustrates the dynamic power flow characteristics of the micro-grid comprising a solar PV source, a battery energy storage system (BESS), and time-varying loads. The set of waveforms highlights the coordinated interaction among generation, storage, and demand under changing operating conditions.

The PV power waveform remains nearly constant throughout the simulation, indicating stable solar generation. This behavior suggests that the PV system is operating either under constant irradiance conditions or with a fixed active power reference imposed by the control strategy. The absence of noticeable fluctuations confirms that the PV output is largely decoupled from short-term load variations and does not directly participate in fast power balancing during transient events.

In contrast, the BESS power waveform exhibits clear charging and discharging dynamics, reflecting its role as the primary balancing resource in the micro-grid. During periods when the load demand exceeds the available PV generation, the battery delivers power to the system, as indicated by negative power values corresponding to discharging operation. As the system reaches steady-state conditions or when excess PV power becomes available, the BESS transitions into charging mode, absorbing surplus energy. The smooth rise and subsequent settling of the battery power demonstrate the effectiveness of the control algorithm in regulating power flow while maintaining voltage and frequency stability.

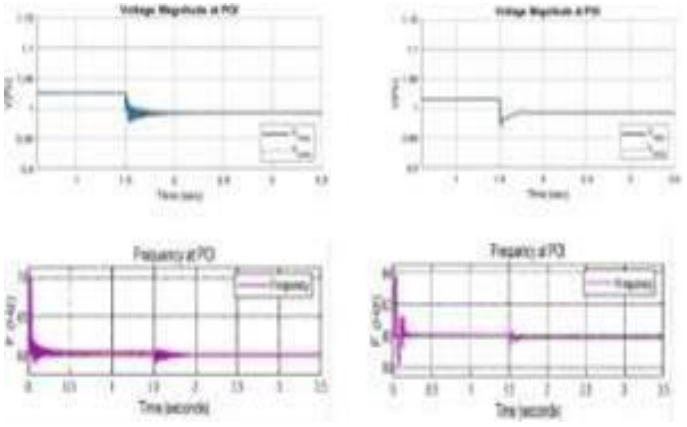

Fig 10. Cont.

The Fig 10.Load power waveform shows distinct step changes corresponding to load switching events. At specific time instants (approximately 0.8 s, 1.2 s, and 1.9 s), the load demand drops sharply to near zero before being reconnected, representing load shedding and restoration scenarios. These abrupt changes introduce transient disturbances in the system, leading to temporary oscillations in the power signals. When the load increases suddenly, the total power demand rises sharply, prompting an immediate response from the BESS to maintain system balance. Conversely, during load reduction, the PV generation momentarily exceeds the demand, causing the BESS to absorb the excess power. Overall, the waveforms in Fig. 9 demonstrate effective coordinated power sharing within the micro-grid. The PV system provides steady generation, while the BESS dynamically compensates for load fluctuations, ensuring smooth power transitions and stable system operation under varying demand conditions.

IJARCCE ISSN (O) 2278-1021, ISSN (P) 2319-5940

International Journal of Advanced Research in Computer and Communication Engineering

Impact Factor 8.471 ⁜ Peer-reviewed & Refereed journal ⁜ Vol. 15, Issue 5, May 2026

DOI: 10.17148/IJARCCE.2026.155248

RESULT

Irradiation	Wind Speed	PV Power	Wind Power	GFM inverter Power
100	5	0.2 MW	15 MW	30 MW
200	5	1.6 MW	15 MW	28 MW
300	5	3.3 MW	15 MW	28 MW
400	5	5 MW	15 MW	28 MW
500	5	7 MW	15 MW	28 MW
600	5	9 MW	15 MW	27 MW
700	5	11 MW	15 MW	28 MW
800	5	13 MW	15 MW	28 MW
900	5	38 MW	15 MW	20 MW
1000	5	50 MW	15 MW	10 MW

Table 1: Effect of Wind speed on PV, Wind & GFM Power.

This Table 1 represents how the total power generation of a hybrid renewable energy system changes with different levels of solar irradiation while keeping the wind speed constant. As irradiation increases from 100 W/m² to 1000 W/m², the PV power output rises significantly, demonstrating the direct relationship between sunlight intensity and photovoltaic generation. For example, at low irradiation of 100 W/m², the PV system generates only 0.2 MW, but as irradiation reaches 1000 W/m², the PV output increases sharply to 50 MW. Throughout all these irradiation levels, the wind speed remains constant at 5 m/s, which means the wind turbine delivers a steady wind power output of 15 MW at every operating point. This constant wind contribution acts as a stable base power source in the hybrid system.

The GFM (Grid Forming) inverter power changes dynamically with increasing solar PV output. At low irradiation levels, the GFM inverter needs to inject more power to maintain system voltage and frequency support— evident from the high value of 30 MW when irradiation is only 100 W/m². As PV generation rises (e.g., 1.6 MW at 200 W/m² or 5 MW at 400 W/m²), the GFM power requirement reduces slightly and stabilizes around 28 MW, showing that the inverter supplies supportive power only to fill the gap between renewable generation and load/grid demands. At very high irradiation levels, when PV generation becomes extremely large such as 38 MW at 900 W/m² and 50 MW at 1000 W/m², the renewable sources contribute more than enough to meet system needs. As a result, the GFM inverter output drops significantly to 20 MW at 900 W/m² and further to 10 MW at 1000 W/m², since the system no longer requires large compensating power from the inverter.

Overall, the table illustrates the coordinated behavior of hybrid renewable sources: PV power increases with irradiation, wind power remains constant due to fixed wind speed, and GFM inverter power decreases as PV contribution becomes dominant, balancing the micro-grid and ensuring stable operation across different renewable energy conditions.

Irradiation	Wind Speed	PV Power	Wind Power	GFL inverter Power
800	6	13 MW	16 MW	28 MW
800	7	13 MW	18 MW	27 MW
800	8	13 MW	20 MW	27 MW
800	9	13 MW	22 MW	26 MW
800	10	13 MW	25 MW	26 MW
800	11	13 MW	28 MW	20 MW
800	12	13 MW	32 MW	20 MW
800	13	13 MW	40 MW	18 MW
800	14	13 MW	45 MW	17 MW
800	15	13 MW	50 MW	16.5 MW

Table 2: Effect of Irradiation on PV, Wind & Power.

DOI: 10.17148/IJARCCE.2026.155248

The Table 2 illustrates the operational behavior of the hybrid renewable energy system when the solar irradiation is maintained at a constant level of 800 W/m². Under this condition, the photovoltaic (PV) system delivers a fixed power output of 13 MW across all operating points, indicating stable solar generation due to unchanged irradiance.

As the wind speed increases from 6 m/s to 15 m/s, the wind power output rises significantly, reflecting the nonlinear, approximately cubic relationship between wind speed and turbine power. At a wind speed of 6 m/s, the wind turbine produces 16 MW, which increases progressively with wind speed, reaching 25 MW at 10 m/s and 32 MW at 12 m/s. A more pronounced increase occurs at higher wind speeds, where wind generation rises to 40 MW at 13 m/s and attains a maximum of 50 MW at 15 m/s. This increase in wind power substantially enhances the total renewable contribution to the micro-grid.

In response to the growing wind generation, the power output of the grid-following (GFL) inverter decreases gradually. At lower wind speeds, the inverter supplies a higher level of support to compensate for limited renewable generation, delivering 28 MW at 6 m/s. As wind power increases, the inverter contribution reduces to approximately 27 MW at moderate wind speeds and further declines to 26 MW at 9–10 m/s. Beyond this point, a sharper reduction is observed, with the inverter output dropping to 20 MW at 11–12 m/s and decreasing further to 18 MW, 17 MW, and finally 16.5 MW at the highest wind speeds.

Overall, these results demonstrate that the GFL inverter operates as a balancing resource within the micro-grid. It provides greater power support when renewable generation is low and progressively reduces its contribution as wind power becomes dominant, thereby ensuring stable and reliable micro-grid operation under constant solar irradiation conditions.

III. CONCLUSION

In this work, grid-forming inverter-based control is developed and implemented in a solar PV system- and BESS-integrated micro grid network. The proposed model is tested under different operating conditions: varying solar irradiation, varying demand conditions, islanded mode and grid faults. The GFM-based inverter control provides an immediate response to the system and reduces switching transients, maintaining the reliability and stability of the system. The FRT capability is incorporated in the control of GFL and GFM inverters, and the system performances are compared. It is understood from the results under different test conditions that GFM control offers increased voltage and frequency stability. The proposed control strategy for renewable-fed inverters achieves a lower rate of change of frequency under system disturbances. The GFM-based inverter control achieves a reduced current limit, and the steady state is achieved quickly, which leads to increased fault-clearing time. In the future works, the authors will concentrate on the development of implementing soft computing approaches for GFM-based inverter control. The GFM based inverter control will be studied in terms of the transient and small signal stability of the system.

REFERENCES

[1] Fang, J.; Li, H.; Tang, Y.; Blaabjerg, F. Distributed power system virtual inertia implemented by grid-connected power converters. *IEEE Transactions on Power Electronics* 2018, *33*, 8488–8499.

[2] Peng, Q.; Jiang, Q.; Yang, Y.; Liu, T.; Wang, H.; Blaabjerg, F. On the stability of power electronics-dominated systems: Challenges and potential solutions. *IEEE Transactions on Industry Applications* 2019, *55*, 7657–7670.

[3] Rosso, R.; Wang, X.; Liserre, M.; Lu, X.; Engelken, S. Grid-forming converters: Control approaches, grid synchronization, and future trends—A review. *IEEE Open Journal of Industry Applications* 2021, *2*, 93–109.

[4] Smith, J.W.; Sunderman, W.; Dugan, R.; Seal, B. Smart inverter volt/var control functions for high penetration of PV on distribution systems. In *Proceedings of the IEEE/PES Power Systems Conference and Exposition*; Phoenix, AZ, USA, 20–23 March 2011; pp. 1–6.

[5] Mittal, R.; Miao, Z. Analytical model of a grid-forming inverter. In *Proceedings of the IEEE Power & Energy Society General Meeting (PESGM)*; Denver, CO, USA, 17–21 July 2022; pp. 1–5.

[6] Kikusato, H.; Ustun, T.S.; Hashimoto, J.; Otani, K.; Nagakura, T.; Yoshioka, Y.; Maeda, R.; Mori, K. Developing power hardware-in-the-loop-based testing environment for volt-var and frequency-watt functions of a 500 kW photovoltaic smart inverter. *IEEE Access* 2020, *8*, 224135–224144.

[7] IEEE Std 1547-2018. *IEEE Standard for Interconnection and Interoperability of Distributed Energy Resources with Associated Electric Power Systems Interfaces*; IEEE: Piscataway, NJ, USA, 2018.

[8] EN 50549-1. *Requirements for Generating Plants to Be Connected in Parallel with Distribution Networks—Part 1: Connection to a LV Distribution Network*; European Committee for Standardization: Brussels, Belgium, 2019.

DOI: 10.17148/IJARCCE.2026.155248

[9] Hoke, A.; Giraldez, J.; Palmintier, B.; Ifuku, E.; Asano, M.; Ueda, R.; Symko-Davies, M. Setting the smart solar standard: Collaborations between Hawaiian Electric and the National Renewable Energy Laboratory. *IEEE Power & Energy Magazine* 2018, *16*, 18–29.

[10] Lasseter, R.H.; Chen, Z.; Pattabiraman, D. Grid-forming inverters: A critical asset for the power grid. *IEEE Journal of Emerging and Selected Topics in Power Electronics* 2020, *8*, 925–935

[11] Yazdani, A.; Iravani, R. *Voltage-Sourced Converters in Power Systems: Modeling, Control, and Applications*; IEEE: Piscataway, NJ, USA, 2010.

[12] Rocabert, A.; Blaabjerg, F.; Rodríguez, P. Control of power converters in AC microgrids. *IEEE Transactions on Power Electronics* 2012, *27*, 4734–4749.

[13] Pattabiraman, D.; Lasseter, R.; Jahns, T. Comparison of grid-following and grid-forming control for a high inverter penetration power system. In *Proceedings of the IEEE Power & Energy Society General Meeting (PESGM)*; Portland, OR, USA, 5–10 August 2018; pp. 1–5.

[14] Zuo, Y.; Yuan, Z.; Sossan, F.; Zecchino, A.; Cherkaoui, R.; Paolone, M. Performance assessment of grid-forming and grid-following converter-interfaced battery energy storage systems on frequency regulation in low-inertia power grids. *Sustainable Energy, Grids and Networks* 2021, *27*, 100496.

[15] Li, Y.; Gu, Y.; Green, T.C. Revisiting grid-forming and grid-following inverters: A duality theory. *IEEE Transactions on Power Systems* 2022, *37*, 4541–4554.

[16] Orihara, D.; Kikusato, H.; Hashimoto, J.; Otani, K.; Takamatsu, T.; Oozeki, T.; Taoka, H.; Matsuura, T.; Miyazaki, S.; Hamada, H.; et al. Contribution of voltage support function to virtual inertia control performance of inverter-based resources in frequency stability. *Energies* 2021, *14*, 4220.

[17] González, I.; Calderón, A.J.; Folgado, F.J. IoT real-time system for monitoring lithium-ion battery long-term operation in microgrids. *Journal of Energy Storage* 2022, *51*, 104596.

[18] Davi, M.J.; Oleskovicz, M.; Lopes, F.V. Study on IEEE 2800–2022 standard benefits for transmission line protection in the presence of inverter-based resources. *Electric Power Systems Research* 2023, *220*, 109304.

[19] Van, L.P.; Chi, K.D.; Duc, T.N. Review of hydrogen technologies-based microgrids: Energy management systems, challenges, and future recommendations. *International Journal of Hydrogen Energy* 2023, *48*, 14127–14148.

[20] Mohammed, N.; Udawatte, H.; Zhou, W.; Hill, D.J.; Bahrani, B. Grid-forming inverters: A comparative study of different control strategies in frequency and time domains. *IEEE Open Journal of the Industrial Electronics Society* 2024, *5*, 185–214.

[21] Tabassum, T.; Toker, O.; Khalghani, M.R. Cyber– physical anomaly detection for inverter-based microgrids using autoencoder neural networks. *Applied Energy* 2024, *355*, 122283.

[22] Ahmad, S.; Shafiullah, M.; Ahmed, C.B.; Alowaifeer, M. A review of microgrid energy management and control strategies. *IEEE Access* 2023, *11*, 21729–21757.

[23] Wang, B.; Burgos, R.; Wen, B. Grid-forming inverter control strategy with improved fault ride-through capability. In *Proceedings of the IEEE Energy Conversion Congress and Exposition (ECCE)*; Detroit, MI, USA, 9–13 October 2022;pp. 1–8.

[24] Lin, Y.; Eto, J.H.; Johnson, B.B.; Flicker, J.D.; Lasseter,R.H.; Villegas Pico, H.N.; Seo, G.S.; Pierre, B.J.; Ellis,A. *Research Roadmap on Grid-Forming Inverters*; National Renewable Energy Laboratory (NREL): Golden, CO, USA, 2020.

[25] Ward, L.; Subburaj, A.; Demir, A.; Chamana, M.; Bayne, S.B. Analysis of grid-forming inverter controls for grid-connected and islanded microgrid integration. *Sustainability* 2024, *16*, 2148.

[26] Hart, P.; Lesieutre, B. Energy function for a grid-tied droop-controlled inverter. In *Proceedings of the North American Power Symposium (NAPS)*; Pullman, WA, USA, September 2014; pp. 1–6.

[27] Johnson, B.B.; Sinha, M.; Ainsworth, N.G.; et al. Synthesizing virtual oscillators to control islanded inverters.*IEEE Transactions on Power Electronics* 2016, *31*, 6002–6015.

[28] Sinha, M.; Dörfler, F.; Johnson, B.; et al., Uncovering droop control laws embedded within the nonlinear dynamics of Van der Pol oscillators. *IEEE Transactions on Control of Network Systems* 2017, *4*, 347–358.

[29] Plet, C.A.; Brucoli, M.; McDonald, J.D.F.; et al. Fault models of inverter-interfaced distributed generators: Experimental verification and application to fault analysis. In *Proceedings of the IEEE Power and Energy Society General Meeting (PESGM)*; Detroit, MI, USA, July 2011; pp. 1–8.

[30] Paquette, A.D.; Divan, D.M. Virtual impedance current limiting for inverters in microgrids with synchronous generators. *IEEE Transactions on Industry Applications* 2015, *51*, 1630–1638.

[31] A. D. Paquette and D. M. Divan, "Virtual impedance current limiting for inverters in microgrids with synchronous generators," IEEE Trans- actions on Industry Applications, vol. 51, no. 2, pp. 1630-1638, Mar.-Apr. 2015